Korean J. Chem. Eng., 39(4), 865-875 (2022)
DOI: 10.1007/s11814-021-0982-2

pISSN: 0256-1115
eISSN: 1975-7220

The Pareto optimal robust design of generalized-order PI controllers based on the decentralized structure for multivariable processes

Vo Lam Chuong*,‡, Truong Nguyen Luan Vu*,†, Nguyen Tam Nguyen Truong,‡, and Jae Hak Jung**,†**

*Faculty of Mechanical Engineering, Ho Chi Minh City University of Technology and Education, 01 Vo Van Ngan St., Thu Duc City, Ho Chi Minh City, Vietnam
**School of Chemical Engineering, Yeungnam University, 280 Daehak-Ro, Gyeongsan 38541, Korea
(*Received 27 July 2021 • Revised 27 September 2021 • Accepted 13 October 2021*)

Abstract−This paper proposes an optimal tuning approach for designing robust generalized-order proportional integral (PI) controllers based on the multi-objective optimization problem for multivariable processes. Generalized-order means that the order of the integral term could be an integer order or a fractional one. Due to the sophistication of an MIMO process, the decentralized structure based on the simplified decoupling is addressed to reduce the full matrix controller (n^2 controllers) to the diagonal form (n controllers). Multi-objective particle swarm optimization (MOPSO) is adopted to design a generalized-order PI controller for each diagonal element of the decoupled matrix. The objective functions are to minimize the integrated absolute error (IAE) for both servomechanism and regulator problems which are normally conflicting in terms of system performance. In the first stage, a Pareto front (PF) including the optimal solutions is obtained, then in the second stage, the most appropriate control parameters are chosen from the PF based on the maximum peak of the sensitivity function (M_s). The robustness stability of the whole system (the MIMO one) is finally evaluated to guarantee the applicability of the control structure. Some simulation examples in comparison with other well-known methods are presented to demonstrate the effectiveness of the proposed method.

Keywords: Fraction-order PI Controller, MOPSO Algorithm, Robust Performance, Simplified Decoupling, Pareto Front Optimization

INTRODUCTION

Multivariable processes in which the interactions between their variables are considerable are common in most industrial systems. Normally, there are three approaches to designing controllers for those systems, including decentralized, decoupled, and centralized control. The decentralized control, which is represented by multi-loop PI/PID controllers, is only appropriate to the modest interactive processes [1]. In a system with strong interactions between process variables, centralized control or decoupled control should be suggested. Model predictive control (MPC) is a typical scheme of centralized control that is mostly used on a higher level with a larger sampling time compared to a lower one with a simple PI/PID control loop. Therefore, decoupled control is a favorite choice for many industrial applications. In this work, simplified decoupling is chosen because of its simplicity and robustness [2,3]. Moreover, the realizability problem of decoupling control is solved by using the particle swarm optimization (PSO) algorithm as proposed in [3].

Even with the development of control theory, the proportional-integral-derivative (PID) controller still plays an important role in industrial applications. According to a survey, more than 90 percent of control loops are of the PID type and in the field of process control, with the PI controller in the majority. For example, a typical paper mill in Canada has more than 2000 control loops in which 97 percent use PI control [4,5]. Recently, the fractional-order PID controller (FOPID) which uses the concept of fractional calculus, has received great attention. The researchers stated that the FOPID, known as the generalization of the classical PID controller, has better dynamic performance as well as better robustness compared to the classical one. However, the better the performance, the more complex the tuning rules because of the increasing of control parameters. Currently, researchers have focused on both approaches of integer order and fractional one. And there are numerous methods to design both kinds of controllers [6-13]. However, there is no general approach to decide which order should be used in a specific case. Therefore, in this work, we propose an optimization approach for a general order case. It means that the obtained controller could be an integer order or a fractional one, depending on the dynamic of the process.

There are many works related to design methods of the PI/PID controller as well as the FOPI/FOPID controller which consider optimization problems with concerns for system performance and its robustness. Normally, these methods could be classified into two directions: frequency based-method and time domain-based evolutionary algorithm (EA). In the frequency domain, the methods based Bode's ideal transfer function with three conditions of the gain at the crossover frequency, the phase margin, and the flat phase constraint at the crossover frequency to ensure system robustness. However, this method is only available for single-input single-output

†To whom correspondence should be addressed.
E-mail: vuluantn@hcmute.edu.vn, jhjung@ynu.ac.kr
‡There two authors are equally contributed in this work.

systems and normally, at the same time, it is only considered a servomechanism problem or regulator problem. The robustness, in this case, is guaranteed by using some criteria in the frequency domain, such as maximum sensitive function or maximum complementary function [11-14]. In the second approach, some EAs such as genetic algorithm (GA) and particle swarm optimization (PSO) are used to solve the control design problems [15-18]. In [15], GA is adopted to design the full matrix controller (centralized control) using fractional-order PID for an MIMO system. Due to the complexity of the controller as well as the algorithm, the author only represented two-input, two-output (TITO) processes in the simulation and the system performance is not good compared to other well-known methods. In [16], the authors designed a robust FOPID controller based on the multi-objective optimization (MOO) for first order plus delay time (FOPDT) processes. The method considers necessary aspects of control design including system performance in terms of set-point tracking and disturbance rejection as well as the system robustness with the maximum sensitive function. However, it is only justified by SISO systems, and it also has to use the Nash solution, which is not familiar to most control engineers, to obtain the final control parameters from the PF. In other papers [17,18], the authors also proposed MOO with Pareto optimal solution to design FOPID for some SISO processes. From the review papers, it can be seen that the tuning rules for high-order MIMO processes (3×3 and 4×4) using FOPI/FOPID controllers which guarantee the system performance as well as the robustness are still an open question.

Currently, most available literatures state that the fractional controller provides better system performance as well as better robustness [5,9-18]. However, whether it is always true or depends on the dynamic of the system is still an open question. Normally, when researching the fractional-order controller, researchers tend to force the order of integral or derivative term to be the fractional one to aim at achieving or improving the performance of the controlled system. However, in some cases, the integer order might provide a better performance, especially in an MIMO case which has strong interactions between process variables and increases the complexity of the dynamic of the system. Therefore, in this paper, the multi optimization algorithm is suggested for tuning the general-order PI controller. Apparently, it is still a fractional-order controller but the order is considered as the general one, i.e., an integer order is also a solution of the proposed method. In addition, the performance and robustness are conflicting objectives, so a control designer has to take into account the compromise between those specifications to ensure the applicability of the proposed method. In this work, the maximum sensitive function (M_s) is adopted in the design step to guarantee the robustness of every single loop. The typical range of M_s value of an integer order SISO system is from 1.2 to 2 as stated in [6], and the lower value of M_s, the more robustness of the controlled system. In this work, to obtain the trade-off between system requirements, the range of M_s is chosen from 1.2 to 1.5 for the general order case. Finally, to measure the robustness of the whole MIMO system, the M−Δ structure with the μ-synthesis, structured singular value (SSV), is addressed in the presence of diagonal multiplicative output uncertainty [19,20].

This paper is organized as follows. Section 2 briefly introduces some material and methods that are used in this work, including fractional calculus, the simplified decoupling technique for multivariable processes, and the multi-objective Pareto optimization approach. Some performance criteria and robust stability are also introduced in this section. In section 3, the proposed FOPI controller and the design procedure using multi-objective PSO algorithm are presented. In Section 4, two case studies are investigated to demonstrate the performance of the proposed controller and also compare with other methods. Finally, conclusions are given in Section 5.

THEORY DEVELOPMENT

1. Fractional order Calculus

Fractional calculus is a generalization of ordinary calculus by extending the integration and differentiation order to the non-integer order. It has been developed for a long time as a field of mathematics and has only been applied for control engineering in the last two decades. It presents a fractional operator ${}_aD_t^v$ where a and t are the limits and v is the fractional order ($v \in R$). There are several definitions for the fractional operator but the most commonly used one was proposed by Riemann and Liouville [5]. It is defined as follows:

$$ {}_aD_t^v f(t) = \frac{1}{\Gamma(n-v)} \frac{d}{dt^n} \int_a^t \frac{f(\tau)}{(t-\tau)^{v-n+1}} dt,\ n-1 < v < n \tag{1} $$

where $\Gamma(\bullet)$ represents the Euler gamma function; with a positive v, the fractional operator denotes fractional derivative, and a negative v represents fractional integral.

The Laplace transformation is used for Eq. (1) under the assumption that all initial conditions are zero. Its result has the form given in (2):

$$ L\{ {}_aD_v^t f(t)\} = s^v F(s) \tag{2} $$

To implement the fractional order in applications, the Oustaloup recursive algorithm with finite numbers of poles and zeros is addressed to approximate the fractional-order into integer one in a specific range of frequency $[\omega_b, \omega_h]$. The approximation is described by the following equations:

$$ s^v \cong s^v_{[\omega_b, \omega_h]} \approx K \sum_{k=-N}^{N} \frac{s+\omega'_k}{s+\omega_k} \tag{3} $$

where the zero, pole, and gain can be calculated, respectively, from:

$$ K = \omega_h^v \tag{4} $$

$$ \omega'_k = \omega_b \left(\frac{\omega_h}{\omega_b}\right)^{(k+N+0.5-0.5v)/(2N+1)} \tag{5} $$

$$ \omega_k = \omega_b \left(\frac{\omega_h}{\omega_b}\right)^{(k+N+0.5-0.5v)/(2N+1)} \tag{6} $$

2. Decentralized Structure using Simplified Decoupling

To deal with the interactions of an MIMO process, simplified decoupling control is employed in this work. Consider an *n*-input and *n*-output multivariable process with a stable, square, and multi-delays transfer function matrix which is represented as the following matrix:

$$\mathbf{G}(s)=\begin{bmatrix} g_{11}(s) & g_{12}(s) & \cdots & g_{1n}(s) \\ g_{21}(s) & g_{22}(s) & \cdots & g_{2n}(s) \\ \vdots & \vdots & \vdots & \vdots \\ g_{n1}(s) & g_{n2}(s) & \cdots & g_{nn}(s) \end{bmatrix} \tag{7}$$

where $g_{ij}(s)=g_{ij0}(s)e^{-\theta_{ij}s}$, i, j=1, 2, …, n of which $g_{ij0}(s)$ denotes the physically proper, stable, and delay-fee transfer function. θ_{ij} represents the delay time.

The decoupling technique is to determine a decoupler matrix, **D**(s), to convert the transfer function matrix of the process into a diagonal form, (**Q**(s)=**G**(s)**D**(s)). As mentioned, in this study, the simplified decoupling is chosen, and Truong proposed an extended method to calculate each element of the decoupler matrix as well as the decoupled matrix for a MIMO process as follows [2]:

$$d_{ji}=\frac{C_{ij}}{C_{ii}},\ \ i, j=1, 2, \ldots, n;\ \ i\neq j \tag{8}$$

$$q_{ii}=\frac{g_{ii}}{\Lambda_{ii}} \tag{9}$$

where $\mathbf{C}=(\text{adj}\mathbf{G})^T$, adj**G** is the transpose of its cofactor matrix; $\Lambda_{ii}=[\mathbf{G}\otimes(\mathbf{G}^{-1})^T]_{ii}$, $\otimes$ is the Hadamard or Schur product, element-by-element multiplication.

The diagonal elements of the decoupled process become complicated when the order of the process increases. In this case, some approximation techniques have been used to reduce these elements by proper transfer functions. For that reason the method in the time domain using the PSO algorithm [3] is adopted to deal with this problem of decentralized control.

The general form of the transfer function using for decoupler elements (d_{ij}) and decoupled processes (q_{ii}) is as follows:

$$G(s)=\frac{K(\tau_z s+1)e^{-\theta s}}{(\tau_1 s+1)(\tau_2 s+1)} \tag{10}$$

where τ_1, τ_2 are time constants and they must be positive values, assuming $\tau_1>\tau_2\geq 0$; K is gain; τ_z is a non-negative parameter ($\tau_z\geq\theta$); θ is a delay time.

In Eq. (10), when $\tau_2=\tau_z=0$, it becomes the well-known first order plus delay time (FOPDT), then G(s) can be rewritten in (11):

$$G(s)=\frac{Ke^{-\theta s}}{\tau_1 s+1} \tag{11}$$

3. Multi-objective Pareto Optimization

A generalized multi-objective optimization problem can be defined as follows:

$$\text{Min } \mathbf{F}(\mathbf{x})=[f_1(\mathbf{x}), f_2(\mathbf{x}), \ldots, f_m(\mathbf{x})],\ \mathbf{F}(\mathbf{x})\in R^m \tag{12}$$

$$\text{Subject to: } g_i(\mathbf{x})\leq 0,\ i=1, \ldots, p.$$

$$h_j(\mathbf{x})=0,\ j=1, \ldots, q.$$

where $\mathbf{x}=[x_1, x_2, \ldots, x_n]^T\in R^n$ is the vector of design variables in a decision space; **F**(**x**) is the vector of objective functions in an objective space; $g_i(\mathbf{x})$ and $h_j(\mathbf{x})$ are the inequality and equality constraints vectors, respectively, and these constraints define the feasible region which contains a feasible solution.

Let $\mathbf{u}=[u_1, u_2, \ldots, u_m]^T$ and $\mathbf{v}=[v_1, v_2, \ldots, v_m]^T$ be two vectors in the objective space. **u** is said to dominate **v** if and only if $\forall i\in\{1, 2, \ldots, m\}$, $u_i\leq v_i$ and $u_i<v_i$ for at least one i. A point $\mathbf{x}^*\in R^n$ is called Pareto optimal with respect to all $\mathbf{x}\in R^n$ if there exists a vector $\mathbf{x}\in R^n$ such that **F**(**x**) dominates **F**($\mathbf{x}^*$). It means that the solution $\mathbf{x}^*$ is said to be Pareto optimal (minimal) if no other solution can be found to dominate $\mathbf{x}^*$. The set of all Pareto optimal points is called the Pareto set, denoted by PS. The set of all Pareto objective vectors, PF=$\mathbf{F}(\mathbf{x})\in R^m$, where $\mathbf{x}\in$PS, is called the Pareto front. The optimal solution will be chosen from the **PF** according to the predetermined criteria.

4. System Performance and Robustness

4-1. Integral Absolute Error (IAE) Index

To evaluate the closed-loop performance, the integral absolute error (IAE) criterion is considered, which is defined as

$$IAE=\int_0^T |e(t)|dt \tag{13}$$

where T is a finite time which is chosen for the integral approach steady-state value.

4-2. Total Variation (TV)

To evaluate the magnitude of the manipulated input usage, the total up and down movement of the control signal is considered as

$$TV=\sum_{k=1}^{T} |u(k+1)-u(k)| \tag{14}$$

TV is a good measure of the smoothness of controller output and should be small [1-3].

4-3. Maximum Sensitivity Value

The maximum peak of sensitivity function is defined as

$$M_s=\max_{\omega} |S(j\omega)| \tag{15}$$

where $S=(I+L)^{-1}$, and L is an open-loop transfer function of a controlled system.

M_s is the inverse of the shortest distance from the Nyquist curve of the open-loop function to the critical point (−1, j0). Normally, feedback control improves performance in terms of reducing steady-state error at all frequencies and maintaining closed-loop stability. In general, both for stability and performance, the value M_s should be close to 1 [6,20]. In addition, one may also consider M_s as a robustness measure, and a small value indicates that the stability margin of the control system is large. Therefore, in most of the literature, the typical range M_s is chosen from 1.4 to 2 [10,20]. In this work, to increase the stability margin as well as ensure the performance of the controlled system, the range M_s will be assigned from 1.3 to 1.5 as a constraint in the second stage of the design procedure.

4-4. Robust Stability Analysis

Due to using simplified decoupling, in the design step, only the robustness of every single loop is considered. However, the robustness of the MIMO system is the most important issue in applications. Because the dynamics of real processes usually have many sources of uncertainty, which degrade performance or even instability in the controlled systems. Therefore, in this work, the robust stability is evaluated by considering the multiplicative output uncertainty to the decoupled matrix (**Q**(s)) as shown in Fig. 1 where **Δ**

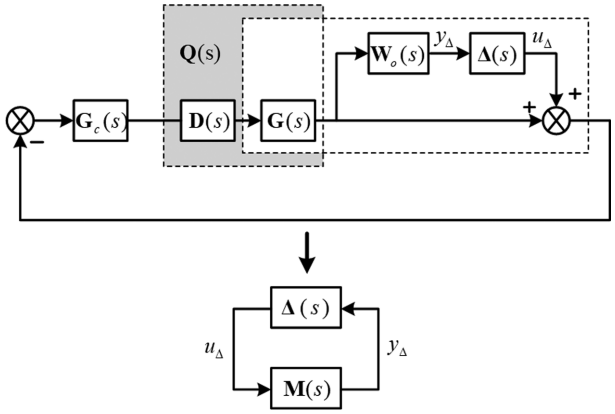

Fig. 1. Robustness stability with multiplicative output uncertainty.

denotes a normalized perturbation with H_∞-norm less than 1 ($\bar{\sigma}(\Delta_i(j\omega))\leq 1\ \forall\omega$, i); $\mathbf{W}_o$(s) is the weight matrix for the output uncertainty.

$\mathbf{Q}(s)=\mathbf{G}(s)\mathbf{D}(s)$: nominal decoupled plant model. (16)

The transfer function matrix from the outputs to the inputs, $\mathbf{M}$(s), can be determined by:

$$\mathbf{M}(s)=\mathbf{W}_o(s)\mathbf{Q}(s)\mathbf{G}_c(s)[\mathbf{I}+\mathbf{Q}(s)\mathbf{G}_c(s)]^{-1} \quad (17)$$

According to the μ-synthesis, the control system will remain stable under multiplicative output uncertainty if the following constraint inequality is satisfied:

$$\mu[\mathbf{M}(j\omega)]=\mu\{\mathbf{W}_o(j\omega)\mathbf{Q}(j\omega)\mathbf{G}_c(j\omega)[\mathbf{I}+\mathbf{Q}(j\omega)\mathbf{G}_c(j\omega)]^{-1}\}<1,\ \forall\omega \quad (18)$$

THE PROPOSED TUNING METHOD

1. The Proposed FOPI Controller

From the equivalent decoupled process transfer function proposed in the previous section, it will be divided into two cases according to Eq. (10) and (11). Then, in this study, a structure of a fractional-order PI controller is proposed for each case and has two following forms, respectively

$$g_c(s)=K_c\frac{1}{s^\sigma}\left(1+\frac{K_I}{s^\lambda}\right) \text{ or} \quad (19)$$

$$g_c(s)=K_c\left(1+\frac{K_I}{s^\lambda}\right) \quad (20)$$

where K_c is the proportional gain; K_I is the integral gain; σ, and λ are the fractional order of integrator ($0<\sigma, \lambda\leq 1$). In Eq. (19) and (20), when $\lambda=1$, the fractional-order becomes the integer one, and then in Eq. (20), it turns out to be the classical PI controller (integer order). Note that integer order controller is also a reasonable solution in this work.

2. The MOPSO Algorithm for the FOPI Controller

As mentioned in the previous section, we used the decoupling technique to transform the transfer function matrix of an MIMO process into a diagonal form. It means that in the controller design step, we just need to deal with each diagonal element independently. Consider a closed-loop control system as in Fig. 2, where g_c is the proposed controller as in (19), and (20); q is a diagonal element of the decoupled process; r, d are the reference input and the disturbance. The parameters of the FOPI are tuned by using the MOPSO algorithm [21,22].

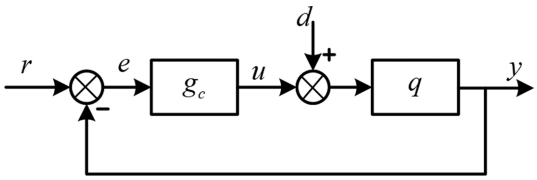

Fig. 2. The closed-loop control system of a single loop.

In the process control field, to evaluate the performance of the control system, we must take into account both problems, including set-point tracking (servomechanism) and disturbance rejection (regulator). For the servomechanism, the system response has to keep tracking to the set-point changes, but for the regulator problem the controller must regulate to stabilize the output at a constant set-point. Therefore, these two objectives conflict in terms of system performance. In most available tuning rules of the PI/PID controller, a good servo tuning may result in a sluggish regulator response and vice versa [16,20]. Therefore, the proposed controller has to be tuned to obtain the compromise between both objective functions. Furthermore, to guarantee the designed controller could be implemented in real applications, the robustness issue must be considered. In this work, the maximum sensitivity, which is defined in (15), is adopted in the design stage to choose the appropriate tuning parameters in the PF.

The MOPSO algorithm using for tuning the proposed FOPI is described as follows:

$$\text{Min } \mathbf{J}(\mathbf{x})=[\mathbf{J}_r(\mathbf{x}), \mathbf{J}_d(\mathbf{x})], \quad (21)$$
$$\text{where } \mathbf{x}=[K_c\ \ K_I\ \ \lambda\ \ \sigma]^T;$$

$\mathbf{J}_r$, $\mathbf{J}_d$ are the IAE index of set-point change and disturbance change, respectively, which is calculated based on Fig. 2 as follows:

$$\mathbf{J}_r=\int_0^\infty |e(t)|dt, \quad d=0 \quad \mathbf{J}_d=\int_0^\infty |e(t)|dt, \quad r=0$$

$$\text{subject to: } \begin{cases} K_{c\,min}<K_c<K_{c\,max} \\ 0<K_I<K_{I\,max} \\ 0.7\leq\lambda\leq 1 \\ 0\leq\sigma\leq 0.3 \end{cases} \quad (22)$$

where $K_{c\,min}$, $K_{c\,max}$, $K_{I\,max}$ are chosen based on the open-loop response of the system. In [23], Chen proposed a guideline to choose the fractional integral order (λ) depending on the dynamic of the first order plus delay time process. In this work, based on that guideline, the boundaries of λ are chosen as $\lambda\in[0.7, 1]$. In [24], $\sigma=1-\lambda$, hence the constraints of $\sigma$are also obtained as in (22) ($\sigma\in[0, 0.3]$).

The tuning procedure is described in Fig. 3. There are two stages: the first one uses the MOPSO algorithm to obtain the PF; then the second stage is run to choose the most appropriate solution from that PF to guarantee the minimization of the set-point tracking error (J_r) using IAE criterion with subject to the proposed range of M_s value.

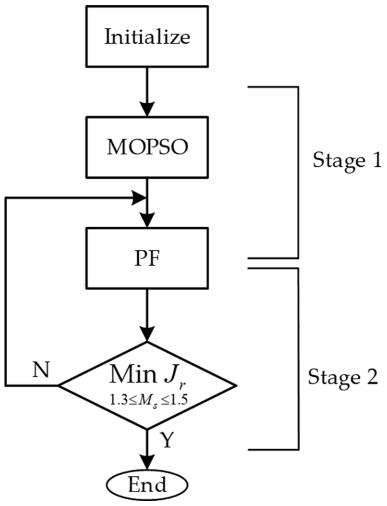

Fig. 3. The flowchart of the proposed method.

Because in the first stage, the minimization of IAE is considered only, which then may lead to poor control performance. It is the reason, in the second stage of the design step, the maximum sensitivity is also taken into account and estimated based on Eq. (15) as follows:

$$M_s \triangleq \max_{\omega \in [\omega_l, \omega_h]} \left| \frac{1}{1+g_c(s)q(s)} \right|_{s=j\omega} \tag{23}$$

SIMULATION STUDY

In this section, two examples of high-order MIMO processes are considered to demonstrate the performance of the proposed method in comparison with those of other well-known methods.

1. The 3×3 MIMO Process: Ogunnaike and Ray (OR) Column

A well-known multi-product distillation column for the separation of a binary ethanol-water mixture studied by many researchers is considered [1-3,25,26]. The open-loop transfer function matrix is given by Eq. (24)

$$\mathbf{G}(s) = \begin{bmatrix} \frac{0.66e^{-2.6s}}{6.7s+1} & \frac{-0.61e^{-3.5s}}{8.64s+1} & \frac{-0.0049e^{-s}}{9.06s+1} \\ \frac{1.11e^{-6.5s}}{3.25s+1} & \frac{-2.36s^{-3s}}{5s+1} & \frac{-0.01e^{-1.2s}}{7.09s+1} \\ \frac{-34.68e^{-9.2s}}{8.15s+1} & \frac{46.2e^{-9.4s}}{10.9s+1} & \frac{0.87(11.61s+1)e^{-s}}{(3.89s+1)(18.8s+1)} \end{bmatrix} \tag{24}$$

The decoupler matrix is obtained as in Eq. (25) [2,3]:

$$\mathbf{D}(s) = \begin{bmatrix} 1 & 0.7549\frac{(0.8337s+1)}{0.533s+1}e^{-0.9s} & 0.0062e^{-0.5233s} \\ 0.3905e^{-2.71s} & 1 & -0.0014 \\ 19.8247\frac{(13.8874s+1)}{8.7956s+1}e^{-8.2s} & -23.1741\frac{(2.0113s+1)}{5.5621s+1}e^{-8.4s} & 1 \end{bmatrix} \tag{25}$$

The diagonal elements of the decoupled matrix are derived as follows [3]:

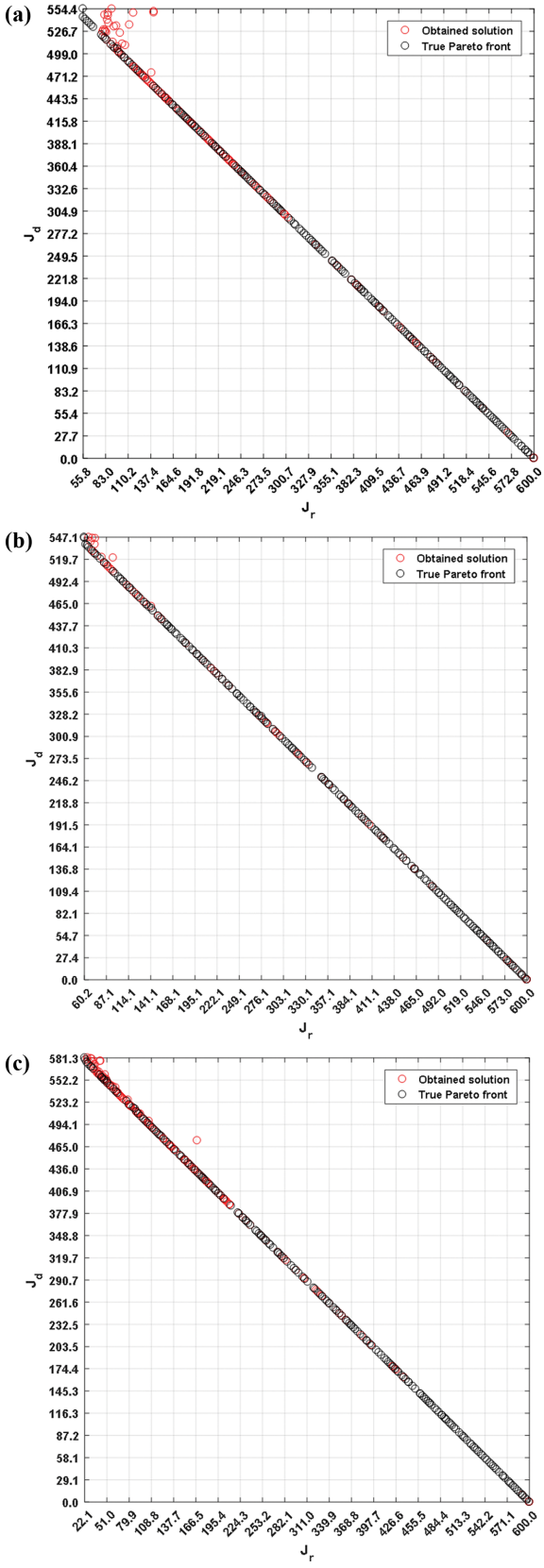

Fig. 4. (a) The PF of two objectives J_r and J_d for the first loop of OR column. (b) The PF of two objectives J_r and J_d for the second loop of OR column. (c) The PF of two objectives J_r and J_d for the third loop of OR column.

Table 1. Controller parameters and resulting performance indices for the OR column

Tuning method	Loops	K_{ci}	K_{Ii}	τ_{Di}	λ_i	σ_i	μ [**M**]	IAE	TV
Proposed	1	1.5043	0.1571	-	1	0.055	0.1002	27.791	4.9783
	2	−0.0896	0.9699	-	0.8321	0.174			
	3	1.3776	0.1073	-	1	0.01			
Multi-loop	1	2.25	0.140	2.58	-	-	0.2479	39.993	6.1432
	2	−0.49	0.1553	3.37	-	-			
	3	4.83	0.3215	10.16	-	-			
CPI	-				-	-	0.1276	25.727	4.9336
	-		$^*\mathbf{G}_c(s)$		-	-			
	-				-	-			

$$^*\mathbf{G}_c(s)=\begin{bmatrix} 1.31+\frac{0.354}{s} & -0.0135-\frac{0.0582}{s} & 0.0207+\frac{0.0026}{s} \\ 0.149+\frac{0.138}{s} & -0.147-\frac{0.0773}{s} & -0.009-\frac{0.0006}{s} \\ 43.6+\frac{6.8}{s} & -9.52+\frac{1.79}{s} & 4.03+\frac{0.421}{s} \end{bmatrix}$$

$$q_{11}=\frac{0.3298(23.1802s+1)e^{-2.6s}}{(21.1355s+1)(3.7363s+1)} \tag{26}$$

$$q_{22}=\frac{-1.2973e^{-3s}}{(1.2739s+1)(0.5014s+1)} \tag{27}$$

$$q_{33}=\frac{0.5601(17.4859s+1)e^{-s}}{(20s+1)(2.6915s+1)} \tag{28}$$

In this case, the diagonal elements of the decoupled matrix have the form as Eq. (10), hence, the proposed controller will have the form as (19). Similar to the previous example, the design procedure includes two steps: the first one is to obtain the PF and then choose the appropriate solution in the second one. Fig. 4(a), (b), and (c) illustrate the results of the PF according to two objectives J_r and J_d (set-point change and disturbance rejection) of the FOPI controllers of every single loop. From these PFs, the second stage of the design procedure is applied to choose the most suitable solution to ensure system performance and robustness. The control parameters are obtained and summarized in Table 1.

In this example, the proposed method is compared with those of decentralized control, which are multi-loop PI/PID controllers [1] and centralized PI controller (CPI) method based on frequency response approximation [26]. In the simulation, the sequential step changes of the set-point were made at t=0, t=200, and t=400 to the loop 1, 2, and 3, respectively. And in the results, Fig. 5(a), (b), and (c) indicate that the proposed controller provides better performance in terms of set-point tracking and disturbance rejection. Disturbance rejection performance was also evaluated by considering the mutual effects of sequential changes on loops 1, 2, and 3. And from those figures, it is clear that the proposed controller gives the least effect, i.e., lowest in the magnitude of variations and fastest recovering times. In addition, some performance indices are also tabulated in Table 1 that prove the effectiveness of the proposed method. There are similar values of IAE and TV of the proposed controller and the CPI method, but the proposed one has the simpler control matrix, including three FOPI controllers compared to the control matrix with nine PI controllers. Fig. 6(a), (b), and (c) illustrate the control signals of every control loop. It can be seen that, in loop 3, the magnitude of manipulated variables is much smaller than that of other methods, which means the proposed controller has the least energy consumption in comparison with other methods in this case.

To demonstrate the robust performance of the proposed method, the μ-synthesis given by Eq. (18) is considered under the assumption of multiplicative output uncertainty. The weight matrix is chosen as:

$$\mathbf{W}_o(s)=\mathrm{diag}\left\{-\frac{s+0.2}{0.5s+1},-\frac{s+0.2}{0.5s+1},-\frac{s+0.2}{0.5s+1}\right\} \tag{29}$$

for the three control loops of the decoupled system. The weight matrix may approximately represent a 20% gain error. Fig. 7 shows the structured singular value (SSV), which is used to evaluate the robust stability of the controlled system. It can be seen that the proposed method still ensures robust stability, while other methods have a peak of μ over 1, which means the controlled system yields instability at that modeling error.

2. The 4×4 MIMO Process: Temperature Control for a Four-room HVAC Process

Well-known temperature control for a four-room heating, HVAC process [2,29] is represented by the open-loop transfer function matrix (4×4) as in (30):

$$\mathbf{G}(s)=\begin{bmatrix} \frac{-0.098e^{-17s}}{122s+1} & \frac{-0.036e^{-27s}}{149s+1} & \frac{-0.014e^{-32s}}{158s+1} & \frac{-0.017e^{-30s}}{155s+1} \\ \frac{-0.043e^{-25s}}{147s+1} & \frac{-0.092e^{-16s}}{130s+1} & \frac{-0.011e^{-33s}}{156s+1} & \frac{-0.012e^{-34s}}{157s+1} \\ \frac{-0.012e^{-31s}}{153s+1} & \frac{-0.016e^{-34s}}{151s+1} & \frac{-0.102e^{-16s}}{118s+1} & \frac{-0.033e^{-26s}}{146s+1} \\ \frac{-0.013e^{-32s}}{156s+1} & \frac{-0.015e^{-31s}}{159s+1} & \frac{-0.029e^{-25s}}{144s+1} & \frac{-0.108e^{-18s}}{128s+1} \end{bmatrix} \tag{30}$$

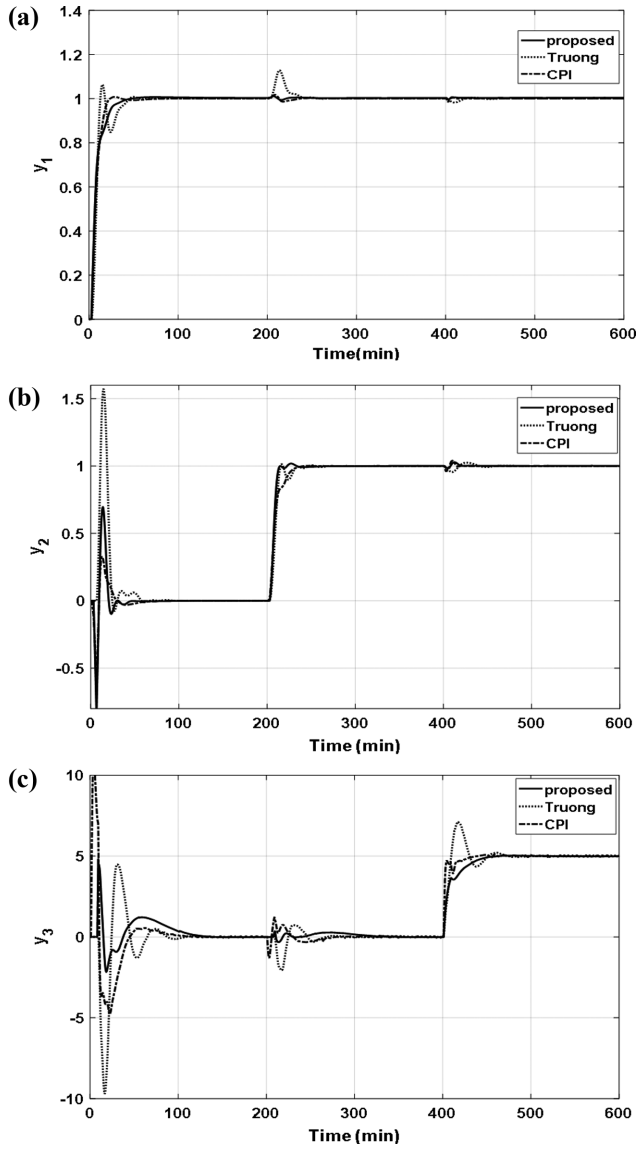

Fig. 5. (a) Closed-loop responses to the unit step change in the set-point of the first loop. (b) Closed-loop responses to the unit step change in the set-point of the second loop. (c) Closed-loop responses to the step change in the set-point of the third loop.

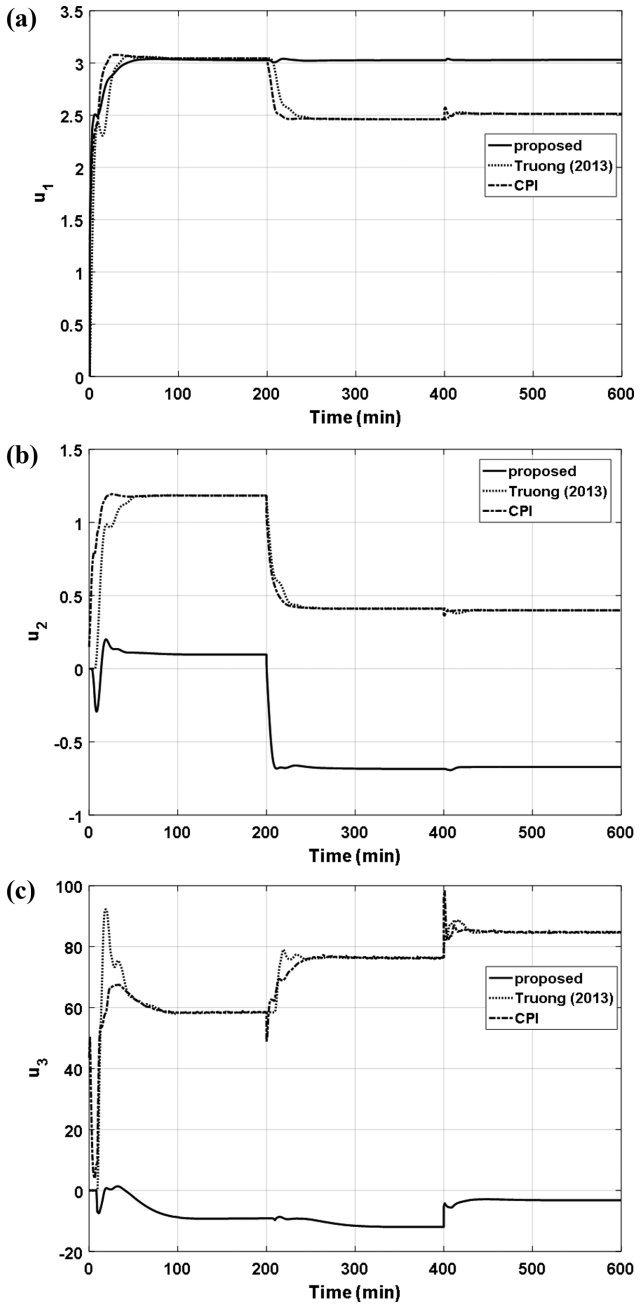

Fig. 6. (a) The control signals to the step change of loop 1. (b) The control signals to the step change of loop 2. (c) The control signals to the step change of loop 3.

The elements of the decoupler matrix are obtained as Eq. (31) [2]:

$$\mathbf{D}(s)=\begin{bmatrix} 1 & \dfrac{-0.341(121.918s+1)e^{-9.151s}}{146.753s+1} & \dfrac{-0.081(132.251s+1)e^{-11.943s}}{164.976s+1} & \dfrac{-0.457(130.872s+1)e^{-8.77s}}{147.641s+1} \\ \dfrac{-0.457(130.872s+1)e^{-8.77s}}{147.641s+1} & 1 & \dfrac{-0.049(235.202s+1)e^{-12.986s}}{228.983s+1} & \dfrac{-0.04(188.514s+1)e^{-14.432s}}{170.865s+1} \\ \dfrac{-0.03(187.93s+1)}{175s+1} & \dfrac{-0.093(97.617s+1)e^{-15.187s}}{117.144s+1} & 1 & \dfrac{-0.304(118.386s+1)e^{-9.165s}}{145.037s+1} \\ \dfrac{-0.049(1946.796s+1)e^{-11.409s}}{1946.775s+1} & \dfrac{-0.073(152.319s+1)e^{-6.741s}}{166.805s+1} & \dfrac{-0.252(124.823s+1)e^{-6.104s}}{138.501s+1} & 1 \end{bmatrix} \quad (31)$$

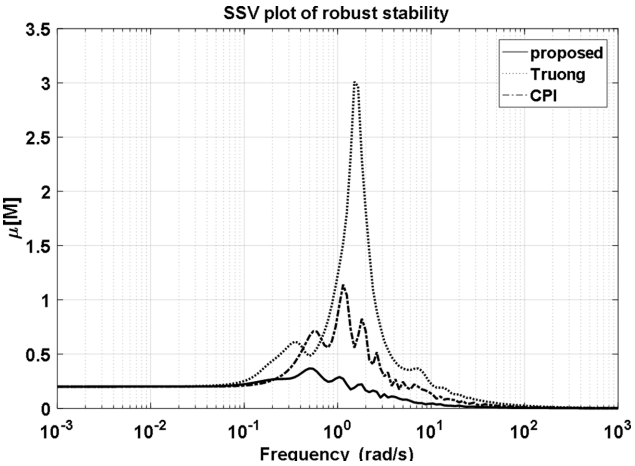

Fig. 7. The SSV plots for robust stability in OR column.

The approximation technique using the PSO algorithm in [3] is applied to derive the diagonal elements of the decoupled matrix. The results are given in the following Eqs. (32)-(35):

$$q_{11}=\frac{-0.0804e^{-17s}}{109.0896s+1} \tag{32}$$

$$q_{22}=\frac{-0.0736e^{-16s}}{117.2055s+1} \tag{33}$$

$$q_{33}=\frac{-0.092e^{-16s}}{112.2966s+1} \tag{34}$$

$$q_{44}=\frac{-0.097e^{-18s}}{121.0125s+1} \tag{35}$$

It is obvious that the diagonal elements have the form as Eq. (11), hence the proposed controller used in this exampled will be

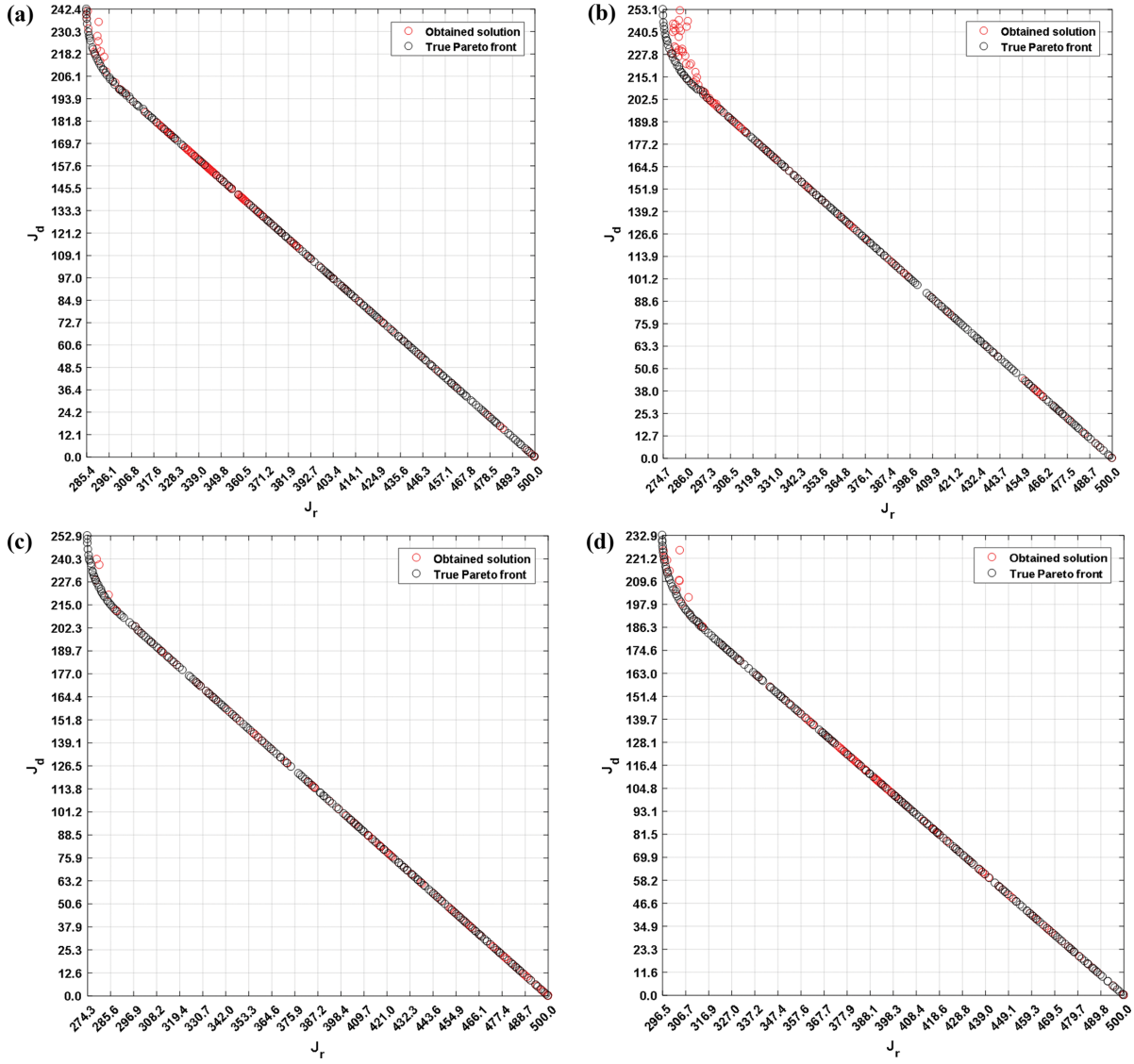

Fig. 8 (a) The PF of two objectives J_r and J_d for the first loop of HVAC process. (b) The PF of two objectives J_r and J_d for the second loop of HVAC process. (c) The PF of two objectives J_r and J_d for the third loop of HVAC process. (d) The PF of two objectives J_r and J_d for the fourth loop of HVAC process.

Table 2. Controller parameters and resulting performance indices for the HVAC system

Tuning method	Loops	K_{ci}	K_{Ii}	λ_i	σ_i	μ [**M**]	IAE	TV
	1	−23.7993	0.0094	1	-			
Proposed	2	−37.2916	0.0091	1	-	0.2019	199.719	207.146
	3	−28.0364	0.0099	1	-			
	4	−26.8817	0.0085	1	-			
				-	-			
1-ODP	-	$\mathbf{G}_{c\text{-}1ODP}(S)^{*}$		-	-	0.2287	372.025	340.492
				-	-			
				-	-			
CPI	-	$\mathbf{G}_{c\text{-}CPI}(s)^{**}$		-	-	0.1999	376.603	200.588
				-	-			

$$
{}^{*}\mathbf{G}_{c\text{-}1ODP}(s)=\begin{bmatrix}
-32.53\left(1+\frac{1}{91.157s}\right) & 12.446\left(1+\frac{1}{75.416s}\right) & 2.234\left(1+\frac{1}{66.442s}\right) & 3.283\left(1+\frac{1}{80.355s}\right)\\
16.218\left(1+\frac{1}{78.425s}\right) & -38.986\left(1+\frac{1}{86.553s}\right) & 1.771\left(1+\frac{1}{87.834s}\right) & 1.535\left(1+\frac{1}{107.734s}\right)\\
1.328\left(1+\frac{1}{97.604s}\right) & 0.9663\left(1+\frac{1}{81.324s}\right) & -32.075\left(1+\frac{1}{86.027s}\right) & 8.297\left(1+\frac{1}{77.120s}\right)\\
1.928\left(1+\frac{1}{87.526s}\right) & 3.016\left(1+\frac{1}{92.745s}\right) & 2.4819\left(1+\frac{1}{80.59s}\right) & -29.268\left(1+\frac{1}{96.763s}\right)
\end{bmatrix}
$$

$$
{}^{**}\mathbf{G}_{c\text{-}CPI}(s)=\begin{bmatrix}
-24.2-\frac{0.219}{s} & 6.86+\frac{0.0808}{s} & 1.09+\frac{0.0158}{s} & 1.88+\frac{0.0205}{s}\\
8.53+\frac{0.100}{s} & -28.1-\frac{0.237}{s} & 1.01+\frac{0.0095}{s} & 0.909+\frac{0.0071}{s}\\
0.815+\frac{0.0066}{s} & 1.85+\frac{0.0221}{s} & -22.1-\frac{0.194}{s} & 4.76+\frac{0.0539}{s}\\
1.06+\frac{0.0107}{s} & 1.68+\frac{0.0172}{s} & 4.59+\frac{0.0489}{s} & -22.0-\frac{0.178}{s}
\end{bmatrix}
$$

as Eq. (20). Similar to example 1, the Pareto fronts are obtained in the first stage as in Fig. 8(a), (b), (c) and (d), and then the second stage is executed to choose the most appropriate control parameters of every single loop from those PFs. The obtained results are listed in Table 2 along with the performance indices of the proposed method and two other approaches. In this example, the centralized PI controller (CPI) design method proposed by Ghosh and Pan [26] and the optimal detuning approach (1-ODP) suggested by Khandelwal and Detroja [28] are addressed here. From Table 2, it can be seen that the orders of the integral term are integer order (λ=1) which means, in this case, the optimal controllers for the HVAC process are the classical PI controllers (integer-order PI controllers).

In the simulation, the sequential step changes of the set-point were made at t=0 (s), t=500 (s), t=1,000 (s), and t=1,500 (s) to the loops 1, 2, 3, and 4, respectively. When there is a step change in a control loop, it is also considered as a load disturbance to other loops. Fig. 9(a), (b), (c), and d demonstrate that the proposed controller provides superior performance in terms of servomechanism and regulator problems over other methods. In addition, some performance indices summarized in Table 2 also show the effectiveness of the proposed method. The μ value is similar to the CPI method, but the proposed controller has a much better IAE index compared to the other methods.

The manipulated signals are shown in Fig. 10(a), (b), (c), and (d) corresponding to the loops 1, 2, 3, and 4 of HVAC process respectively. It is obvious that the proposed method has smoother control signals compared to other methods. Moreover, at the timing of sequence changes of the set-point (t=0, 500, 1,000, and 1,500 second), there are no effects to these signals while, in other methods, sudden changes also happen at those times, especially in the 1-ODP method. As a result of that, the TV index in Table 2 of the 1-ODP method is significantly larger than that of other methods. The proposed method and CPI method have almost the same value of this index.

In this example, the weight matrix is chosen similarly to example 1 (approximately ±20% modeling error):

$$
\mathbf{W}_o(s)=\mathrm{diag}\left\{-\frac{s+0.2}{0.5s+1},-\frac{s+0.2}{0.5s+1},-\frac{s+0.2}{0.5s+1},-\frac{s+0.2}{0.5s+1}\right\} \tag{36}
$$

for the four control loops of the decoupled system. Fig. 11 illustrates the μ plots of three methods that guarantee robust stability in the presence of multiplicative output uncertainties.

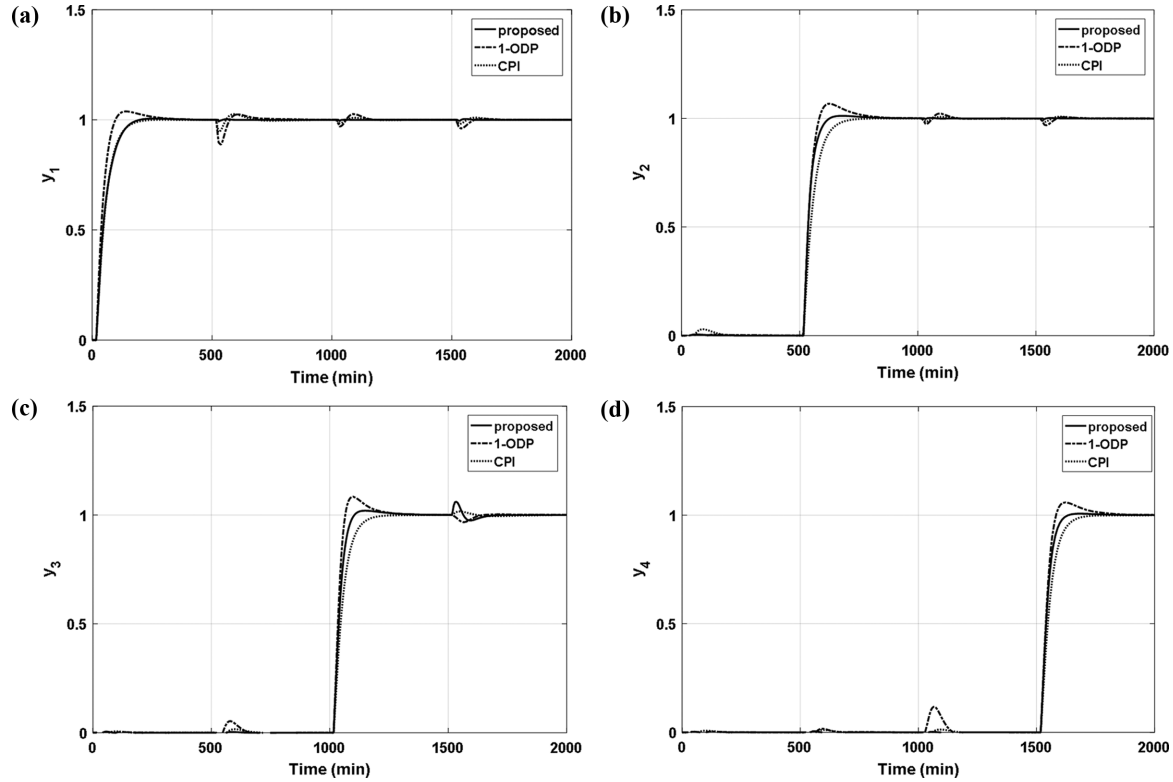

Fig. 9. (a) Closed-loop responses to the unit step change in the set-point of loop 1. (b) Closed-loop responses to the unit step change in the set-point of loop 2. (c) Closed-loop responses to the unit step change in the set-point of loop 3. (d) Closed-loop responses to the unit step change in the set-point of loop 4.

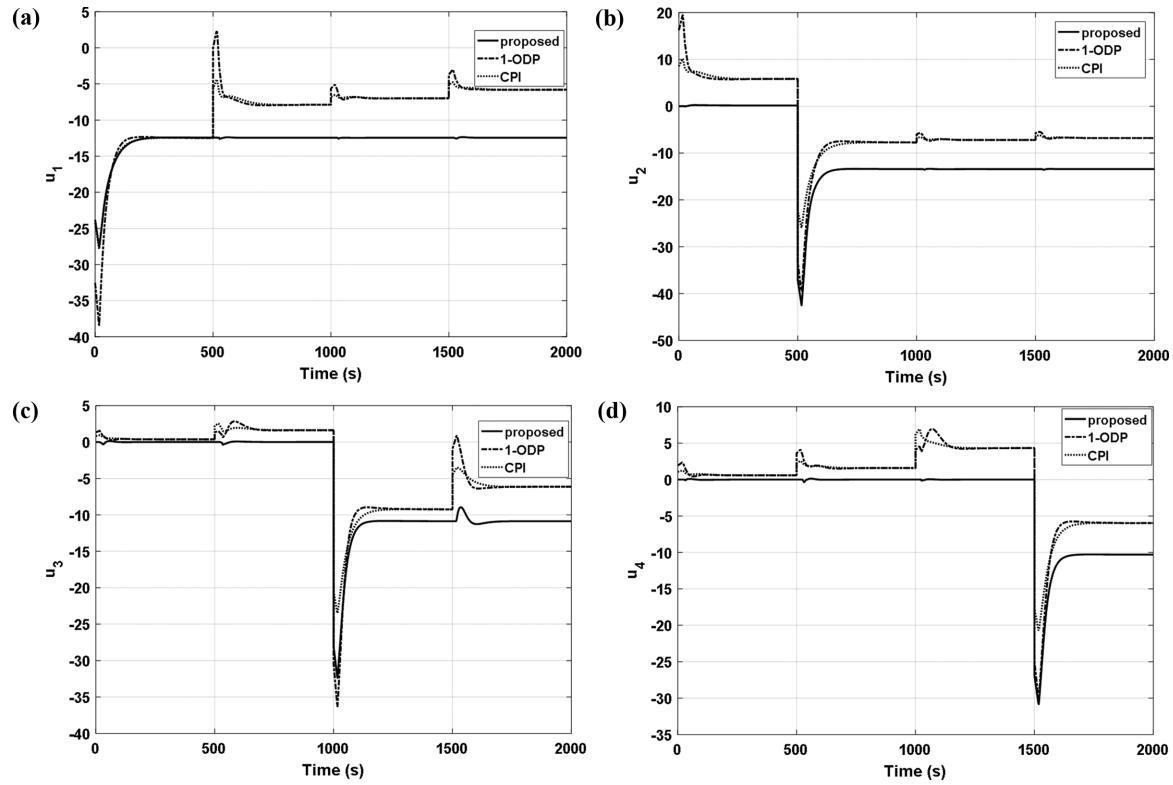

Fig. 10. (a) The control signals for the step change of loop 1. (b) The control signals for the step change of loop 2. (c) The control signals for the step change of loop 3. (d) The control signals for the step change of loop 4.

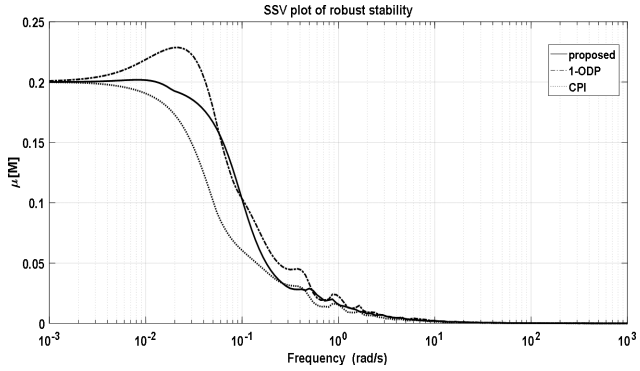

Fig. 11. The SSV plots for robust stability in HVAC process.

CONCLUSIONS

A robust optimal design approach for multivariable processes is proposed by using the decoupling technique and MOPSO algorithm in combination with well-known robust criteria, maximum sensitive function. The fractional-order PI controller, in this work, is considered as a general case of the classical PI controller. That means the optimal solution could be fractional order or the integer one, depending on the degree and dynamic of the controlled processes. The effectiveness and robustness of the proposed method are testified by two simulations of high-order MIMO processes (3×3 and 4×4 processes). In general, the obtained results demonstrate the superior performance of the proposed approach over other methods in both problems of process control, which are servomechanism and regulator, as well as ensure the robustness of the controlled systems. The robust stability is justified by multiplicative output uncertainties with the choice of the weight matrix that represents approximately ±20% of the modeling error. The simulations prove that the proposed method still performs satisfactorily with better output responses in most examples.

ACKNOWLEDGEMENTS

This research was funded by Ho Chi Minh City University of Technology and Education through the project number T2021-24TD and supported by Yeungnam University.

REFERENCES

1. N. L. V. Truong and M. Lee, *J. Chem. Eng. Japan*, **43**, 196 (2010).
2. N. L. V. Truong and M. Lee, *J. Chem. Eng. Japan*, **46**, 279 (2013).
3. V. L. Chuong, T. N. L. Vu, N. T. N. Truong and J. H. Jung, *Appl. Sci.*, **9**, 2487 (2019).
4. W. L. Bialkowski, *Pulp Pap.*, **11**, 19 (1994).
5. Y. Q. Chen, I. Petras and D. Xue, *Fractional order control - a tutorial*, American Control Conference (2009).
6. K. J. Astrom, H. Panagopoulos and T. Hagglund, *Automatica*, **34**(5), 585 (1998).
7. T. H. Kim, I. Maruta and T. Sugie, *Automatica*, **44**, 1104 (2008).
8. R. Vilanova, O. Arrieta and P. Ponsa, *ISA Trans.*, **81**, 177 (2018).
9. A. A. Dastjerdi, B. M. Vinagre, Y. Q. Chen and H. HosseinNia, *Annu. Rev. Control*, **47**, 51 (2019).
10. F. Padula and A. Visioli, *J. Process Control*, **21**, 69 (2011).
11. T. N. L. Vu and M. Lee, *ISA Trans.,* **52**, 583 (2013).
12. R. D. Keyser, C. I. Muresan and C. M. Ionescu, *ISA Trans.,* **62**, 268 (2016).
13. E. Yumuk, M. Guzelkaya and I. Eksin, *ISA Trans.*, **91**, 196 (2019).
14. M. Beschi, F. Padula and A. Visioli, *Cont. Eng. Pra.*, **60**, 190 (2016).
15. M. Moradi, *J. Process Control*, **24**, 336 (2014).
16. H. S. Sánchez, F. Padula, A. Visioli and R. Vilanova, *ISA Trans.*, **66**, 344 (2017).
17. A. Hajiloo, N. Nariman-zadeh and A. Moeini, *Mechatronics*, **22**, 788 (2012).
18. I. Pan and S. Das, *Int. J. Electr. Power Energy Syst.*, **43**, 393 (2012).
19. M. Morari and E. Zafiriou, *Robust process control*, Englewood Cliffs, Prentice Hall (1989).
20. S. Skogestad and I. Postlethwaithe, *Multivariable feedback control analysis and design*, John Wiley & Sons (1996).
21. C. A. C. Coello and M. S. Lechuga, CEC'02 (Cat. No. 02TH8600), USA, **2**, 1051 (2002)
22. C. A. C. Coello, G. T. Pulido and M. S. Lechuga, *IEEE Trans. Evo. Comp.*, **8**(3), 256 (2004).
23. C. A. Monje, Y. Q. Chen, B. M. Vinagre, D. Y. Xue and V. Feliu, *Fractional-order systems and controls, fundamentals and applications*, Springer-Verlag, London (2010).
24. V. L. Chuong, T. N. L. Vu, N. T. N. Truong and J. H. Jung, *Appl. Sci.*, **9**(23), 5262 (2019).
25. B. A. Ogunnaike, J. P. Lemaire, M. Morari and W. H. Ray, *AIChE J.*, **29**, 632 (1983).
26. S. Ghosh and S. Pan, *ISA Trans.*, **110**, 117 (2021).
27. Y. Shen, W.-J. Cai and S. Li, *Cont. Eng. Pra.*, **18**(6), 652 (2010)
28. S. Khandelwal and K. P. Detroja, *J. Process Control*, **96**, 23 (2020).